2022 International Symposium on Power Electronics,
Electrical Drives, Automation and Motion

Supercapacitor Parameter Estimation and Hybridyzation with PEMFC for Purge Compensation

Nayzel I. Jannif
School of Information Technology, Engineering, Mathematics and Physics
The University of the South Pacific
Suva, Fiji
nayzel.jannif@usp.ac.fj

Krishnil Ram
School of Information Technology, Engineering, Mathematics and Physics
The University of the South Pacific
Suva, Fiji
krishnil.ram@usp.ac.fj

Kaluwin Bangalini
School of Information Technology, Engineering, Mathematics and Physics
The University of the South Pacific
Suva, Fiji
kaluwinundu@gmail.com

Andrea Loli
School of Information Technology, Engineering, Mathematics and Physics
The University of the South Pacific
Suva, Fiji
s11151703@student.usp.ac.fj

Ali Mohammadi
School of Information Technology, Engineering, Mathematics and Physics
The University of the South Pacific
Suva, Fiji
ali.mohammadi@usp.ac.fj

Maurizio Cirrincione
School of Information Technology, Engineering, Mathematics and Physics
The University of the South Pacific
Suva, Fiji
maurizio.cirrincione@usp.ac.fj

2022 International Symposium on Power Electronics, Electrical Drives, Automation and Motion (SPEEDAM) | 978-1-6654-8459-6/22/$31.00 ©2022 IEEE | DOI: 10.1109/SPEEDAM53979.2022.9842176

***Abstract*—This paper focuses on the hybridization of a Proton Exchange Membrane Fuel Cell (PEMFC) and a Supercapacitor to smoothen the voltage disturbance caused by purging in the Fuel Cell. Firstly, a two-branch supercapacitor (SC) model is implemented in Simulink. The parameters of the SC are estimated using Genetic Algorithm Optimization and compared with the classical Faranda method. There is good agreement with the results generated using the Genetic Algorithm Optimization approach. Additionally, experiments were carried out on a 1.2kW PEMFC to acquire the voltage data. Voltage drops during purge were measured and used with the PEMFC model to simulate purge behaviour in the fuel cell. The SC was then connected in parallel to the PEMFC to smoothen the voltage output. The work is still in progress, and so far, positive results have been achieved where the SC has been effective in negating the effects of purge phenomena in PEMFC.**

Keywords— Fuel Cell, Supercapacitor, Hybrid Systems, Parameter Estimation, Genetic Algorithm, Purge, PEMFC

I. INTRODUCTION

Climate change and global warming are affecting the islands, especially the low-lying atolls, in the Pacific and other parts of the world. One of the main factors is the pollution which is generated by the combustion of fossil fuels for transportation and electricity production [1]. According to the study by the World Energy Outlook in 2016 [2], fossil fuels had been generating 85% of air-borne pollution that was emitted into the atmosphere. However, due to the increasing effects of climate change globally, renewable energy is becoming an urgent tool to help end the reliance on fossil fuels as the main source of energy [3].

The idea of the development of fuel cells (FC) has evolved since the 1800s till 1955, when Thomas Grubb and Leonard Niedrach made an advanced modification on the FC producing the Polymer Electrolyte Membrane Fuel Cell (PEMFC) [4]. PEMFCs powered by hydrogen gas (or in liquid form) have become one of the most promising clean energy to be developed because of their zero-emission attribute and environmental friendliness [5]. A PEMFC is an electrochemical device used to generate electricity which uses hydrogen as the main fuel source mixed with oxygen/air in a chemical reaction to produce electricity. Water (H_20) is the main waste product terminated from this chemical reaction with unused nitrogen gas. PEMFC have become an attractive technology in the transportation sector because of its high power density, solid membrane, and lower operating temperature [6],[7]. Due to its numerous advantages, many transportation industries are interested in manufacturing vehicles, buses, and cars that use hydrogen as their fuel [8].

Further advancement in compressing the thickness of Membrane Electrode Assembly (MEA) has become a vital issue for current losses due to nitrogen build-up and excess water in the membrane. Therefore, the "Purging Process" is used to exhaust the build-up of nitrogen gases and also rebalance the water (or remove the excess water) in the FC.

During the purging process, there is a temporary shut-down of the FC which affects its performance [9]. Whenever purging starts, the voltage will immediately drop until the purging process is completed.

A large amount of literature have been published on the purging strategy of the PEMFC. An online hydrogen sensor was developed in [10] with an electromagnetically operated purging valve that controls the hydrogen content during purging. Similarly, [11] involved the same idea of supplying hydrogen for the system to obtain a constant anode pressure during the purging process. In [11], when purging occurs, it forces the exhaust valve to open so the nitrogen and excess water can be removed, which results in a pressure drop at the anode volume. Also [11] proposed using an Iterative Learning Control (ILC) strategy to control this adverse effect. The research also endorsed the Optimal Learning Control (OLC) strategy for the same pressure and concluded that ILC was the best strategy to employ when multiple purging occurs. Also, the OLC strategy should be employed during the fast convergence of purging.

In comparison to the strategy of energy management for the pressure at the anode, work done in [12] derived a method of improving pressure distribution on the MEA which resulted in better handling of flooding problem during the Dead-end mode. In addition, [13] discussed another strategy based on high-temperature dynamic performance. A model was developed based on the transient characteristics of the high-temperature PEMFC voltage and a fuzzy controller that controls the purging schedule at the actual time when there were changes in load.

Authorized licensed use limited to: University of the South Pacific. Downloaded on October 03,2022 at 23:25:55 UTC from IEEE Xplore. Restrictions apply.

According to [12], increasing the period of closing the valve (from 5s to 10s) results in more voltage fluctuations. Experimental work and analysis from [14] were used to approximate the duration of optimal purging as 0.2s. The duration of purging is the time when the valve is open while the purge interval refers to the time when the valve is closed. Researchers in [15] utilized the purge interval using the current density. They used 25% nitrogen concentration to activate the purge interval and concluded that the purge interval can be controlled and adjusted in regards to the changes in current load. Besides, the purge interval at a current density of 0.4 A/cm^2 can be extended for 520s. The same idea of current density was proposed by [16]. Their finding concluded that the back diffusion of water improves the performance recovery time after purging. Thus, increasing the current density reduces the performance recovery time after purging.

Although many published papers discuss the strategy for purging, the gap of voltage drop during the duration of purge discussed above is a vital issue to address. According to the literature, most of them discuss the control strategy of energy management of PEMFCs dealing with dynamic load changes. One of the control strategies of the voltage uniformity of the load changes in a FC is to adjust the current step amplitude and the current variation of frequency. Experiments were done in [17] proving that the current step amplitude should be reduced while the current variation frequency is increased as much as possible to attain a uniform voltage during dynamic loading.

Additionally, the SC and battery can store energy and be utilized with the PEMFC to supplement any voltage transient during the variation of loads [18],[19]. For decades, batteries have been the preferred storage devices, mainly because of their ability to store high energy density. But the downside is it takes very long to discharge and recharge, which limits its ability to deliver power. The focus these days is on SCs also known as an ultracapacitor or double-layered capacitor which holds the discharge characteristics of a capacitor and the energy storage properties of a battery. Jayalakshmi et al. [20] had proposed in using SC as a secondary source to supply or absorb the power during load changes. Work done by [20] implemented a current control strategy to balance the power by using load current as a reference compared with the energy source current. Another study conducted by Partridge and Bucknall [21] addressed a similar scenario. They developed in a similar system but with a control strategy that kept the FC voltage constant while the SC supplemented for the load transient.

SCs have been used in many applications to compensate for the power fluctuations, including PEMFCs. FCs are usually integrated with other auxiliary energy sources such as batteries and/or SCs. These configurations are usually called hybrid systems. Many of the configurations of the hybrid system employed by the literature consist of DC-DC converters that provide the control of the FC system. Work done in [22],[23] focuses on the stability of FC output and SC to supplement FC during high power transient. The scheme discussed by [22],[23] employs an FC coupled in parallel with a SC with two DC-DC converters. The boost converter works as a unidirectional converter to maintain the constant output voltage of the system. The buck-boost converter works in a bidirectional way where the buck mode charges the SC while the boost mode supplies the energy to the system when needed. This scheme gives a reference current that is subtracted from the load current, which gives the signal to the SC and buck-boost to adjust itself to meet the load demand continually.

In comparison, [6],[24] also have a similar configuration of a FC-SC hybrid system with two DC-DC converters. However, the authors of [6],[24] used the state of charge (SOC) of the SC to recover energy loss. Their algorithm operates in the charging mode when SOC is less than 60% and discharge mode when SOC is greater than 60%. The SOC is mainly used with the application of the vehicle. Thus, the mode of operation discussed was obtained when the vehicle is at the acceleration, braking, and stopping phase. The SC discharges when it supplies the energy during acceleration mode where the FC was not connected. Likewise, it charges up during the deceleration of the vehicle. During deceleration, the energy generated from braking was used to charge up the SC while the FC was not connected.

Furthermore, there is also the passive configuration of the FC-SC hybrid system as discussed by [25]. The passive system is somewhat a good choice for the users of the FC applications due to its affordable costs. It is cheaper compared to utilizing DC-DC converters with the FC but has a disadvantage that cannot respond to the fast transient peak power demand. Therefore, using the DC-DC converter coupled with the FC and SC maintains the output voltage at a desired level.

This paper presents a Passive FC-SC Purge compensation scheme simulated using actual experimental FC purge data. Firstly, an FC experimental rig is setup to capture FC purge data which will be later used in simulations. Secondly, in order to simulate the SC response to the FC purge phenomena, the parameters of the SC are estimated. The SC parameters are identified utilizing a separate experiment by recording its current and voltage data and then applying a classical method as well as an optimization algorithm. Finally, the FC-SC hybrid scheme is simulated with actual FC experimental data in conjunction with a SC model with parameters representing a real SC.

The paper is organized as follows: Section II presents the modelling and experimental rig of the PEMFC, Section III describes the 2-branch model of the SC and the experimental rig and methods used to identify it's parameters and Section IV presents the proposed FC-SC hybrid scheme with the results.

II. Descritpion, Modelling and Experimental Rig of the PEMFC

A. Experimental setup for PEMFC

A 1.2 kW open cathode PEMFC was loaded using a DC electronic load, as shown in Fig 1. Data was collected from the PEMFC user interface module. A single ramp current load was programmed into the electronic load, starting at 2A and ending at 60A. The PEMFC was not able to output a current lower than 2A. Voltage and current were logged in the Electronic load as well. The sampling rate in both cases are 2Hz.

Authorized licensed use limited to: University of the South Pacific. Downloaded on October 03,2022 at 23:25:55 UTC from IEEE Xplore. Restrictions apply.

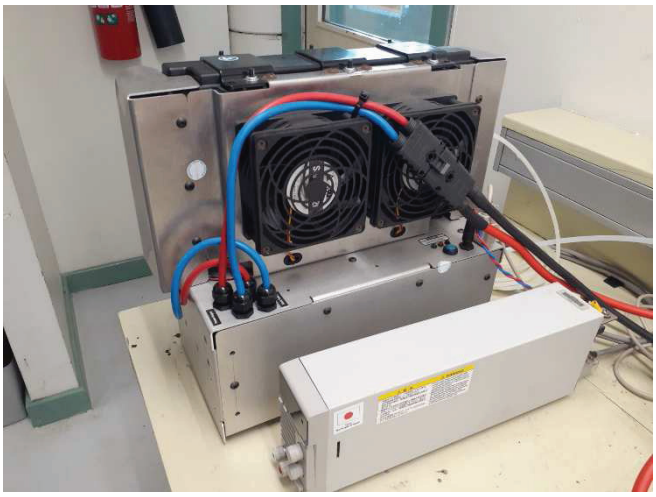

Fig. 1. Experimental setup of 1.2kW PEMFC

The Simulink model was run for 100s and the resulting polarization curve (Fig. 2) was compared to the measured experimental data. The PEMFC used to gather the experimental results had 28 cells with a maximum voltage reaching 0.9 V in each cell. The PEMFC area was 62 cm^2 while its membrane thickness was 0.42mm. Parameter estimation was carried out using nonlinear least squares method. The parameter estimation details are stated in [26]

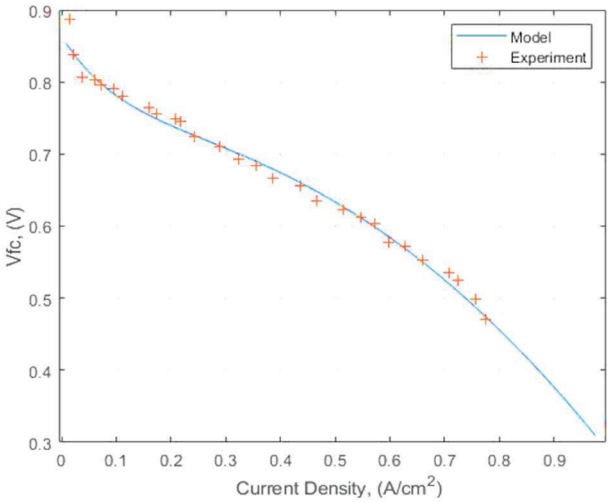

Fig. 2. Experimental and model results compared

Generally, there is good agreement between the polarization curve estimated through the model and the results obtained through experiments.

B. PEMFC model

The Nernst voltage or the theoretical voltage potential the PEMFC can develop at a certain pressure of hydrogen and oxygen is given by:

$$E = 1.229 - 0.85 \times 10^{-3}(T - 298.15) + 4.3085 \times 10^{-5}\, T\left[\ln(p_{H_2}) + \frac{1}{2}\ln(p_{O_2})\right] \quad (5)$$

While the Nernst voltage provides the theoretical maximum voltage, there are several voltage losses which occur in the PEMFC to reduce the actual output voltage for the cells:

$$v_{fc} = E - (v_{act} + v_{ohm} + v_{conc}) \quad (6)$$

These losses arise from three areas – activation losses, ohmic losses and concentration losses. The activation losses arise due to energy requirements for breaking the bonds and the sluggish rate of reactions at the electrode surface [27].

$$v_{act} = v_0 + v_a(1 - e^{-c_1 i}) \quad (7)$$

where v_a, v_o and c_1 are constants that need to be estimated as shown in [26]. The resistance of electron flow for conducting electrodes and the resistance of ion flow for the membrane results in ohmic losses:

$$v_{ohm} = i\, R_{ohm} \quad (8)$$

where R_{ohm} is the internal resistance of the PEMFC. The concentration voltage losses v_{conc} arise due to concentration gradients as the reactants get used up at the cell surfaces and the slow transport of reactants to and from the reaction sites. This can be computed as:

$$v_{conc} = i\left(c_2 \frac{i}{i_{max}}\right)^{c_3} \quad (9)$$

The reactant flow dynamics in the PEMFC are used in equation 9 to estimate the total theoretical voltage that can be generated by each cell. The reactant gas flow changes in line with the demand current, which can be assumed to be the only input into the system.

III. SC Modelling and Parameter Estimation

A. The 2-Branch SC Model

A SC can be described by suitable circuits modelling its terminal behaviour and numerous models are discussed in literature [28],[29]&[30]. Among these the Classical Model, Non-Linear Capacitance Model, 3-branch model, 4-branch model, ladder model and transmission line model [28],[29]&[30]. This paper focuses on the 2-branch model by Faranda [12] sketched in Fig. 3 for its simplicity and ease of analysis.

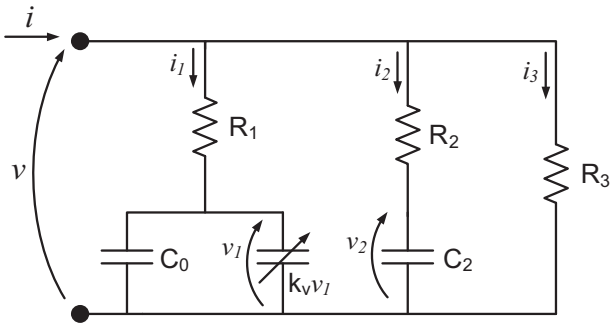

Fig. 3. 2-branch model of SC.

The 2-branch model is well known since it can accurately characterize the SC behaviour during frequent charging-discharging cycles, which is best suited for EV's applications where this behaviour is exhibited [31].

The 1st branch consists of three components and models the voltage dependency of the capacitance. This branch gives the SC a time constant in the order of seconds. The 2nd branch of the equivalent circuit consists of a resistance in series with a capacitance and models the charge redistribution with a time constant of minutes. The 3rd branch consists of

Authorized licensed use limited to: University of the South Pacific. Downloaded on October 03,2022 at 23:25:55 UTC from IEEE Xplore. Restrictions apply.

one resistor and models the time varying self-discharge, which is modeled as a function of the SC terminal voltage. The state equations of this circuit are

$$\left.\begin{aligned}\frac{dv_1}{dt} &= \frac{1}{C_1 G_{||}}\left[G_1\left(G_1 - G_{||}\right)v_1 + G_1 G_2 v_2 + G_1 i\right] \\ \frac{dv_2}{dt} &= \frac{1}{C_2 G_{||}}\left[G_2\left(G_2 - G_{||}\right)v_2 + G_1 G_2 v_1 + G_2 i\right] \\ v &= \frac{G_1 v_1 + G_2 v_2 + i}{G_{||}}\end{aligned}\right\} \quad (10\ a,b,c)$$

where: $G_i = \frac{1}{R_i}$ $(i = 0,2,3)$, $G_{||} = G_1 + G_2 + G_3$
and $C_1 = C_0 + k_v v_1$

B. Experimental Rig for SC Characterisation

An experimental rig is setup for the purpose of extraction of the SC voltage and current curves. This data are then used further in this research for purpose of parameter identification of the SC.

The SC chosen for the emulation of the proposed FC-SC hybrid model in this paper consisted of a "GreenCap" MH47765 Super Capacitor bank which was constructed using 6 × SC cells connected in series. Each single cell is 500F with a voltage rating of 2.7V shown in Fig. 4.

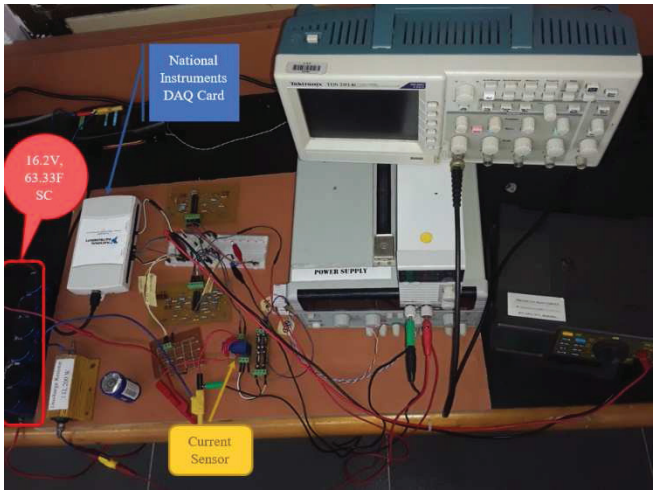

Fig. 4. The SC Experimental Rig for Parameter Estimation

The series configuration has resulted in the net capacitance of the Bank, C_{Bank}, becoming 83.33F. The voltage balancing between the cells is made possible via balancing circuit which were pre-installed by the manufacturer. The voltage rating of the SC Bank is calculated to be 16.2 V. A National Instruments (NI) USB 6211 DAQ system was utilized to capture the voltage and current profile of the SC. The sampling frequency of the setup was 1 kHz.

C. SC Parameter Identification

For the purpose of simulating the FC-SC hybrid scheme in this paper, the parameters of the SC in Section C need to be identified in accordance with the Faranda 2-branch model. This is achieved by two of the following means:

(1.) By strictly following the methodology as laid out by Faranda in [30]; and
(2.) Further verification of the above by means a Computational Intelligence method, specifically by the use of a Minimisation Algorithm – Genetic Algorithm (GA).

GAs have been proved to have the advantages for demonstrating strong robustness, searching and simple processing in many studies, and they are appropriate for searching the ideal parameters of SC models. The GA has three optimization factors, which are the optimization objective, optimization variables and constraint criterion.

The State Space equations in (10) are simulated on the Simulink Platform of Matlab by a random population generated by the GA, which results in it's voltage and current variables giving a unique set of values for each iteration of the algorithm. In each iteration, these are compared against the experimental voltage and current of the SC. In doing so, an error function is realized by the use of the Root Mean Square Error. The objective of the GA is to minimize the error.

Similar work was done by Wang et. al. [32] and Miniguano [33] however, none of the models have the non-linearity constraint as per the 2-branch model (Fig. 3) utilized in this paper. The results show agreement between the 2 methods as shown in Table 1 and in the Graph comparing experimental with simulated voltage curves in Fig. 5.

TABLE 1: TWO BRANCH MODEL PARAMETERS

Parameters	Faranda Parameters	GA Parameters	|% Error|
R_1 (Ω)	0.15	0.15	0.00
C_0 (F)	41.03	40.74	0.71
K (F/V)	2.29	1.70	25.76
R_2 (Ω)	22.59	22.31	1.24
C_2 (F)	29.56	11.24	61.98
R_3 (Ω)	70,000	70,000	0.00

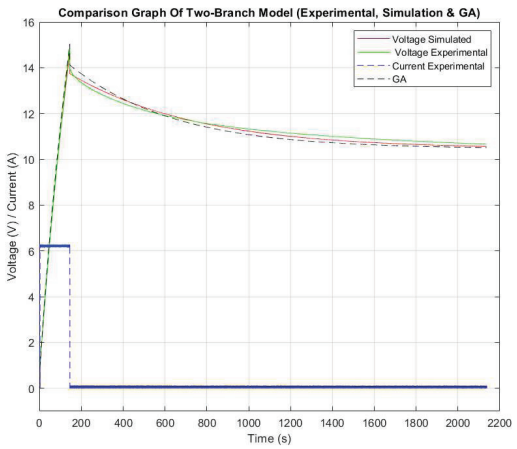

Fig. 5. Two Branch Modelling Output.

The voltage graph of the estimated SC parameters are simulated and compared with the experimental curve shown in Fig. 5 are analyzed for Goodness of Fit. Finally, the Root Mean Square Error (RMS error) of the GA and Faranda

Authorized licensed use limited to: University of the South Pacific. Downloaded on October 03,2022 at 23:25:55 UTC from IEEE Xplore. Restrictions apply.

voltage curves compared against the experimental voltage curve were found to be 0.3939 and 0.46 respectively.

IV. FC-SC Hybrid Scheme, Results and Discussion

A. FC-SC Hybrid Scheme

The FC-SC hybrid systems have been studied by many researchers resulting in many different topologies. Most of the topologies studied have been discussed in the Introduction. This paper will analyze the passive topology as shown in Fig. 6. The idea of the development of this topology is obtained from the article [34],[35],[36]&[37] and justified in the Section I.

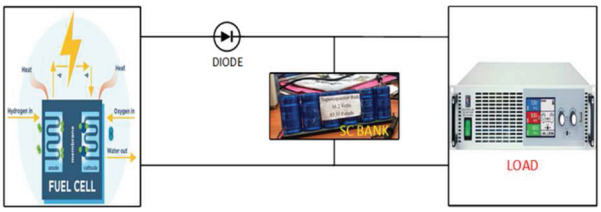

Fig. 6. Passive topology – Direct coupling of PEMFC and SC

The topology in Fig. 6 shows the SC connected in parallel with the PEMFC with a dynamic load attached. The system is a passive FC-SC hybrid configuration defined without any DC/DC converters, which makes the power distribution inherently decided by the characteristics of the FC and the SC. In this case, each device has to be properly sized to have equal potential, since any potential difference would result in resistance and attract current flow. Usually, when there is resistance, it forces electric charges to move from lower potential to higher potential. Therefore, a diode is placed in front of the FC to prevent the possible charging of the stack from the SCs in case of Open Circuit Potential of the FC stack dropping below that of the SC [38].

B. FC Purge

Fig. 7 shows the purge data derived from experimental results of the 1.2kW PEMFC. The voltage drop occurs to flush out the unused excess gases from the PEMFC. The voltage drops significantly during this phase as there are no reactant material to generate voltage. At t = 52 s the voltage drops from 23.2V to 0.5 V. This is 97.8% drop in the voltage during purge. The sudden drop in voltage is too large to be compensated for by a DC-DC converter.

A. FC-SC Purge Compensation Results

Fig. 8 shows the voltage after compensation by the proposed FC-SC hybrid scheme. The SC easily compensates the voltage drop and while voltage ripples exist at the purge instances, these drops are minor. A DC-DC converter and can be handled these minor ripples. Looking at t = 52 s, the voltage drop is from around 23.2 V to 21.5 V. This is a voltage drop of around 7.3% only compared to the 97.8% drop with a purge compensation scheme. The purge compensation scheme works even in the case of load changes.

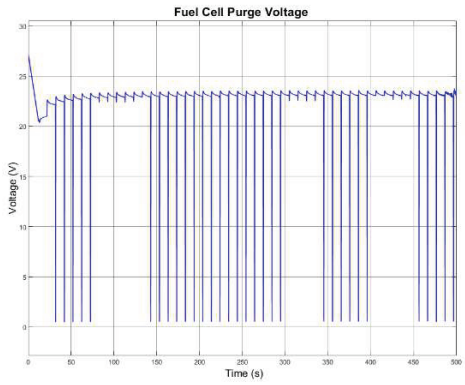

Fig. 7. Purge results determined experimentally and modelled in Simulink

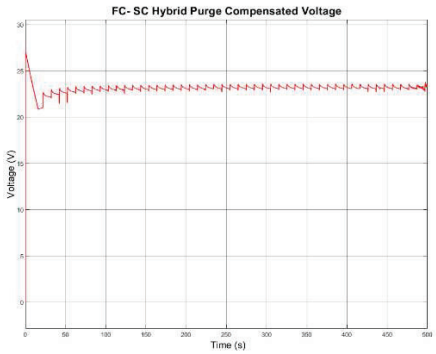

Fig. 8. Voltage results after purge compensation using the FC-SC scheme.

V. Conclusion

This paper presents how to compensate for the voltage drop when the purge process occurs in the PEM fuel cell. In this, the SC as parallelly connected to the fuel cell as a charge reservoir to make up for the voltage drop. Three schemes of the FC-SC hybrid system were developed and analyzed. The FC-SC passive topology was implemented having the fuel cell purge data in place of the PEM fuel cell due to test the theory. The results from the simulation included the polarization curve with accounted losses from the fuel cell, and also the charging and discharging voltage waveform of the SC. The final results with the SC connected in parallel with the PEMFC show a clear smoothing effect on the voltage drops caused by purging in the PEMFC. While there are some voltage ripples remaining, these can be accounted for using a DC-DC converter which will be looked at in future.

References

[1] "Energy and exergy analysis of fuel cells_ A review | Elsevier Enhanced Reader." https://reader.elsevier.com/reader/sd/pii/S2451904918302749?token=CCB73B6FC139851F804FAC169C75397BBDE8939788585DF62D8A031011E90A518145452FC50D67CBE564BF5CF9B75C2E&originRegion=us-east-1&originCreation=20220309234209 (accessed Mar. 10, 2022).

[2] J. M. Andújar and F. Segura, "Fuel cells: History and updating. A walk along two centuries," *Renew. Sustain. Energy Rev.*, vol. 13, no. 9, pp. 2309–2322, Dec. 2009, doi: 10.1016/j.rser.2009.03.015.

[3] A. Madoh, J. Alenazi, L. Alkhamees, and A. Panwar, "Case Study on Market Mix Strategies of Toyota Motor Corporation," *Asia Pac. J. Manag. Educ.*, vol. 2, no. 3, Art. no. 3, Nov. 2019, doi: 10.32535/apjme.v2i3.630.

[4] F. Perera, "Pollution from Fossil-Fuel Combustion is the Leading Environmental Threat to Global Pediatric Health and Equity: Solutions Exist," *Int. J. Environ. Res. Public. Health*, vol. 15, no. 1, Art. no. 1, Jan. 2018, doi: 10.3390/ijerph15010016.

Authorized licensed use limited to: University of the South Pacific. Downloaded on October 03,2022 at 23:25:55 UTC from IEEE Xplore. Restrictions apply.

[5] D. J. N. S, D. N. Gaonkar, and P. B. Nempu, "Power Control of PV/Fuel Cell/Supercapacitor Hybrid System for Stand-alone Applications," *Int. J. Renew. Energy Res. IJRER*, vol. 6, no. 2, Art. no. 2, Jun. 2016.

[6] I. OECD, "Energy and Air Pollution: World Energy Outlook Special Report 2016," 2016. http://www.iea.org/publications/freepublications/publication/weo-2016-special-report-energy-and-air-pollution.html (accessed Mar. 10, 2022).

[7] A. Ahmed, A. Q. Al-Amin, A. F. Ambrose, and R. Saidur, "Hydrogen fuel and transport system: A sustainable and environmental future," *Int. J. Hydrog. Energy*, vol. 41, no. 3, pp. 1369–1380, Jan. 2016, doi: 10.1016/j.ijhydene.2015.11.084.

[8] C. Hähnel and J. Horn, "Iterative Learning Control of a PEM fuel cell system during purge processes," in *2016 IEEE International Energy Conference (ENERGYCON)*, Apr. 2016, pp. 1–6. doi: 10.1109/ENERGYCON.2016.7513874.

[9] M. Rahimi-Esbo, A. Ramiar, A. A. Ranjbar, and E. Alizadeh, "Design, manufacturing, assembling and testing of a transparent PEM fuel cell for investigation of water management and contact resistance at dead-end mode," *Int. J. Hydrog. Energy*, vol. 42, no. 16, pp. 11673–11688, Apr. 2017, doi: 10.1016/j.ijhydene.2017.02.030.

[10] B. Chen, Z. Tu, and S. H. Chan, "Performance degradation and recovery characteristics during gas purging in a proton exchange membrane fuel cell with a dead-ended anode," *Appl. Therm. Eng.*, vol. 129, pp. 968–978, Jan. 2018, doi: 10.1016/j.applthermaleng.2017.10.102.

[11] A. Rabbani and M. Rokni, "Effect of nitrogen crossover on purging strategy in PEM fuel cell systems," *Appl. Energy*, vol. 111, pp. 1061–1070, Nov. 2013, doi: 10.1016/j.apenergy.2013.06.057.

[12] Y. Li, X. Zhao, Z. Liu, Y. Li, W. Chen, and Q. Li, "Experimental study on the voltage uniformity for dynamic loading of a PEM fuel cell stack," *Int. J. Hydrog. Energy*, vol. 40, no. 23, pp. 7361–7369, Jun. 2015, doi: 10.1016/j.ijhydene.2015.04.058.

[13] M. G. Carignano, R. Costa-Castelló, V. Roda, N. M. Nigro, S. Junco, and D. Feroldi, "Energy management strategy for fuel cell-supercapacitor hybrid vehicles based on prediction of energy demand," *J. Power Sources*, vol. 360, pp. 419–433, Aug. 2017, doi: 10.1016/j.jpowsour.2017.06.016.

[14] T. C. Do *et al.*, "Energy Management Strategy of a PEM Fuel Cell Excavator with a Supercapacitor/Battery Hybrid Power Source," *Energies*, vol. 12, no. 22, Art. no. 22, Jan. 2019, doi: 10.3390/en12224362.

[15] W. Wu, J. S. Partridge, and R. W. G. Bucknall, "Simulation of a stabilised control strategy for PEM fuel cell and supercapacitor hybrid propulsion system for a city bus," *Int. J. Hydrog. Energy*, vol. 43, no. 42, pp. 19763–19777, Oct. 2018, doi: 10.1016/j.ijhydene.2018.09.004.

[16] Q. Jian, L. Luo, B. Huang, J. Zhao, S. Cao, and Z. Huang, "Experimental study on the purge process of a proton exchange membrane fuel cell stack with a dead-end anode," *Appl. Therm. Eng.*, vol. 142, pp. 203–214, Sep. 2018, doi: 10.1016/j.applthermaleng.2018.07.001.

[17] L. Bai, F. Li, Q. Hu, H. Cui, and X. Fang, "Application of battery-supercapacitor energy storage system for smoothing wind power output: An optimal coordinated control strategy," in *2016 IEEE Power and Energy Society General Meeting (PESGM)*, Jul. 2016, pp. 1–5. doi: 10.1109/PESGM.2016.7741798.

[18] G. Dotelli, R. Ferrero, P. Gallo Stampino, S. Latorrata, and S. Toscani, "Supercapacitor Sizing for Fast Power Dips in a Hybrid Supercapacitor—PEM Fuel Cell System," *IEEE Trans. Instrum. Meas.*, vol. 65, no. 10, pp. 2196–2203, Oct. 2016, doi: 10.1109/TIM.2016.2549658.

[19] C. Dépature, A. Macías, A. Jácome, L. Boulon, J. Solano, and J. P. Trovão, "Fuel cell/supercapacitor passive configuration sizing approach for vehicular applications," *Int. J. Hydrog. Energy*, vol. 45, no. 50, pp. 26501–26512, Oct. 2020, doi: 10.1016/j.ijhydene.2020.05.040.

[20] D. Arora, M. Hinaje, C. Bonnet, S. Raeel, and F. Lapicque, "Sizing Supercapacitor for Direct Hybridization with Polymer Electrolyte Membrane Fuel Cell," in *2018 IEEE Vehicle Power and Propulsion Conference (VPPC)*, Aug. 2018, pp. 1–7. doi: 10.1109/VPPC.2018.8605027.

[21] D. Arnaudov, V. Dimitrov, and P. Punov, "Analytical Model for Supercapacitor Sizing as Part of a Hybrid Power Supply," in *2019 IEEE 60th International Scientific Conference on Power and Electrical Engineering of Riga Technical University (RTUCON)*, Oct. 2019, pp. 1–5. doi: 10.1109/RTUCON48111.2019.8982362.

[22] N. Hinov, G. Vacheva, and Z. Zlatev, "Modelling a charging process of a supercapacitor in MATLAB/Simulink for electric vehicles," *AIP Conf. Proc.*, vol. 2048, no. 1, p. 060023, Dec. 2018, doi: 10.1063/1.5082138.

[23] T.-W. Chun, H.-G. Kim, and E.-C. Nho, "Charging and discharging strategies of grid-connected super-capacitor energy storage systems," in *2018 IEEE International Conference on Industrial Technology (ICIT)*, Feb. 2018, pp. 1743–1747. doi: 10.1109/ICIT.2018.8352446.

[24] K. R. Ram, K. Naidu, R. Kumar, M. Cirrincione, and A. Mohammadi, "Model Comparison and Parameter Estimation of Polymer Exchange Membrane (PEM) Fuel Cell Based on Nonlinear Least Squares Method," in *2019 International Aegean Conference on Electrical Machines and Power Electronics (ACEMP) 2019 International Conference on Optimization of Electrical and Electronic Equipment (OPTIM)*, Aug. 2019, pp. 500–505. doi: 10.1109/ACEMP-OPTIM44294.2019.9007136.

[25] Z. Liu *et al.*, "Anode purge management for hydrogen utilization and stack durability improvement of PEM fuel cell systems," *Appl. Energy*, vol. 275, p. 115110, Oct. 2020, doi: 10.1016/j.apenergy.2020.115110.

[26] M. Serra, J. Aguado, X. Ansede, and J. Riera, "Controllability analysis of decentralised linear controllers for polymeric fuel cells," *J. Power Sources*, vol. 151, pp. 93–102, Oct. 2005, doi: 10.1016/j.jpowsour.2005.02.050.

[27] S. Mobayen and F. Tchier, "Nonsingular fast terminal sliding mode stabilizer for a class of uncertain nonlinear systems based on disturbance observer," *Sci. Iran.*, vol. 24, Sep. 2016, doi: 10.24200/sci.2017.4123.

[28] N. Devillers, S. Jemei, M.-C. Péra, D. Bienaimé, and F. Gustin, "Review of characterization methods for supercapacitor modelling," *J. Power Sources*, vol. 246, pp. 596–608, Jan. 2014, doi: 10.1016/j.jpowsour.2013.07.116.

[29] L. Zubieta and R. Bonert, "Characterization of double-layer capacitors for power electronics applications," *IEEE Trans. Ind. Appl.*, vol. 36, no. 1, pp. 199–205, Jan. 2000, doi: 10.1109/28.821816.

[30] R. Faranda, "A new parameters identification procedure for simplified double layer capacitor two-branch model," *Electr. Power Syst. Res.*, vol. 80, no. 4, pp. 363–371, Apr. 2010, doi: 10.1016/j.epsr.2009.10.024.

[31] N. Reichbach and A. Kuperman, "Recursive-Least-Squares-Based Real-Time Estimation of Supercapacitor Parameters," *IEEE Trans. Energy Convers.*, vol. 31, no. 2, pp. 810–812, Jun. 2016, doi: 10.1109/TEC.2016.2521324.

[32] C. Wang, H. He, Y. Zhang, and H. Mu, "A comparative study on the applicability of ultracapacitor models for electric vehicles under different temperatures," *Appl. Energy*, vol. 196, pp. 268–278, Jun. 2017, doi: 10.1016/j.apenergy.2017.03.060.

[33] H. Miniguano, A. Barrado, C. Fernández, P. Zumel, and A. Lázaro, "A General Parameter Identification Procedure Used for the Comparative Study of Supercapacitors Models," *Energies*, vol. 12, no. 9, Art. no. 9, Jan. 2019, doi: 10.3390/en12091776.

[34] W. Andari, M. S. BEN YAHIA, H. Allagui, and A. Mami, "Modeling and Simulation of PEM Fuel Cell/Supercapacitor hybrid power sources for an electric vehicle," in *2019 10th International Renewable Energy Congress (IREC)*, Mar. 2019, pp. 1–6. doi: 10.1109/IREC.2019.8754584.

[35] W. Wu, J. S. Partridge, and R. W. G. Bucknall, "Stabilised control strategy for PEM fuel cell and supercapacitor propulsion system for a city bus," *Int. J. Hydrog. Energy*, vol. 43, no. 27, pp. 12302–12313, Jul. 2018, doi: 10.1016/j.ijhydene.2018.04.114.

[36] B. Allaoua, K. Asnoune, and B. Mebarki, "Energy management of PEM fuel cell/ supercapacitor hybrid power sources for an electric vehicle," *Int. J. Hydrog. Energy*, vol. 42, no. 33, pp. 21158–21166, Aug. 2017, doi: 10.1016/j.ijhydene.2017.06.209.

[37] A. Wahib, S. Ghozzi, H. Allagui, and A. Mami, "Design, Modeling and Energy Management of a PEM Fuel Cell / Supercapacitor Hybrid Vehicle," *Int. J. Adv. Comput. Sci. Appl.*, vol. 8, Jan. 2017, doi: 10.14569/IJACSA.2017.080135.

[38] "(PDF) Design and testing of a 9.5 kWe proton exchange membrane fuel cell-supercapacitor passive hybrid system." https://www.researchgate.net/publication/261662622_Design_and_testing_of_a_95_kWe_proton_exchange_membrane_fuel_cell-supercapacitor_passive_hybrid_system (accessed Mar. 10, 2022).

Authorized licensed use limited to: University of the South Pacific. Downloaded on October 03,2022 at 23:25:55 UTC from IEEE Xplore. Restrictions apply.